Modeling of the target surface modification by reactive ion implantation during magnetron sputtering

D. Depla[a)]
Department of Solid State Sciences, University of Ghent, Krijgslaan 281 (S1), B-9000 Ghent, Belgium

Z. Y. Chen, A. Bogaerts, and V. Ignatova
Department of Chemistry, University of Antwerp, Universiteitsplein 1, B-2610 Wilrijk-Antwerpen, Belgium

R. De Gryse
Department of Solid State Sciences, University of Ghent, Krijgslaan 281 (S1), B-9000 Ghent, Belgium

R. Gijbels
Department of Chemistry, University of Antwerp, Universiteitsplein 1, B-2610 Wilrijk-Antwerpen, Belgium

The erosion rate of an aluminum target bombarded with Ar^+ and O_2^+ ions was simulated using TRIDYN. An abrupt change of the erosion rate is noticed at a critical mole fraction of O_2^+ ions. This target behavior can also be described by a simple analytical model showing that the abrupt change finds its origin in an avalanche induced by reaction ion implantation. Indeed, by the reduction of the average sputter yield by compound formation, more reactive ions become implanted into the target as the number of implanted ions depends inversely on the average sputter yield. As such, an avalanche situation can develop which finally results in a completely oxidized target. It is also shown that the critical mole fraction depends linearly on the sputter yield of the target material and that target poisoning induced by ion implantation can result in a hysteresis behavior for the target condition. © *2004 American Vacuum Society.* [DOI: 10.1116/1.1705641]

I. INTRODUCTION

During reactive magnetron sputter deposition of oxides, nitrides, carbides, and other compounds, abrupt changes in deposition rate, target voltage, and reactive gas pressure have been noticed by several authors.[1] Several models have been formulated to explain these avalanche-like changes. They describe the dynamic balance between compound formation on the target surface and the compound dissociation by the sputtering process as a function of the reactive gas flow. Under conditions of high pumping speed and low current, these models predict no avalanche-like changes. However, it was shown recently that during reactive sputtering of Si_3N_4,[2] under conditions of high pumping speed and low current, the target voltage changes abruptly at a given critical mole fraction. This effect and other experimental results[3–5] can be explained by a mechanism based on the reactive ion implantation during the magnetron sputter process. The implantation of reactive ions results in the subsurface formation of the compound, which has a lower sputter yield than the original target material. The chemical reaction between the implanted atoms and the target material results therefore in a decrease of the target surface erosion speed, and consequently the surface concentration of the implanted species, which is inversely proportional to the erosion speed, increases, further reducing the erosion speed of the target surface. This mechanism can result in an avalanche-like change of the target surface condition. Recently,[6] the authors have studied this mechanism in detail, using a dynamic Monte Carlo model. The simulation code TRIDYN was applied to simulate the bombardment of Ar^+ and O_2^+ ions on an aluminum target and to investigate the reactive sputtering of aluminum in a magnetron discharge. It was shown that the formation of aluminum oxide always takes first place in the subsurface region. Moreover, we have investigated the calculated erosion rate as a function of the oxygen mole fraction. Besides the expected decrease of the erosion rate, we found an abrupt change in the erosion rate at a mole fraction $f = 0.03$. These numerical results confirm the proposed idea of target poisoning by reactive ion implantation.

In this article, we have used the same simulation code TRIDYN to study this abrupt change of the erosion rate in more detail. We compare the results of these simulations with an analytical model. A first version of this analytical model was used to describe the effect of ion implantation on the target condition during reactive magnetron sputtering.[7] The aim of this article is to verify the validity of this analytical model by comparison with the TRIDYN results.

II. DESCRIPTION OF THE TRIDYN SIMULATIONS

The TRIDYN simulations were described in detail.[6] The effective surface binding energy of Al and O was chosen in dependence on the actual surface composition by use of a matrix method as described by Möller *et al.*[8] Because the incident energy of the reactive ions O_2^+ is very high compared to the dissociation energy of the oxygen molecule, surface collision will cause an immediate dissociation of O_2^+. Therefore, TRIDYN uses half of the incident energy of O_2^+ as the incident energy of the O^+ ions but its fluence is doubled. In these simulations we assume no formation of oxygen molecules in the target and the extra oxygen over the

---

[a)]Electronic mail: diederik.depla@ugent.be

stoichiometry will outdiffuse from the target. A proper fluence increment of 10^{12} ions/pseudoparticle is used, which is a good choice to reduce computer time and to maintain precision. The total applied fluence was chosen to reach steady-state conditions. For convenience of description, let f denote the ratio of the pseudoparticle number of O_2^+ ions to the sum of Ar^+ and O_2^+ ions. Assuming that the ratio of Ar^+ and O_2^+ fluxes is proportional to the ratio of the partial pressure of Ar and O_2, the f is identical to the oxygen mole fraction in the plasma. We realize that chemisorption of the reactive gas on the target and the gettering of the reactive gas by the sputtered Al atoms will also influence the behavior of the reactive sputtering process.[3,7,9] However, the goal of this simulation is to study the effect of ion implantation on the target condition during reactive magnetron sputtering. Therefore, we assume that the oxygen mole fraction in the plasma is known and we neglect the impingement of other species (i.e., O^+, Ar, O_2, and O) than Ar^+ and O_2^+ on the target surface. At this point we wish to mention that several processes which can occur during ion implantation and sputtering are not included in this TRIDYN code, e.g., Gibbsian segregation, radiation-enhanced diffusion, recoil implantation, and others. These processes can have an influence on the oxidation mechanism. However, as stated before, the aim of this article is a comparison between the results of this TRIDYN code and a simple analytical model, which also does not included these effects.

III. RESULTS AND DISCUSSION

A. TRIDYN simulations

The TRIDYN code was used to simulate the bombardment of aluminum by Ar^+ and O_2^+ ions. For different oxygen mole fractions f, we have calculated the surface erosion due to this ion bombardment as a function of the fluence. From such a simulation, the steady-state erosion rate was calculated and its change studied as a function of the oxygen mole fraction. We have performed such a simulation at four different energies, i.e., 180, 360, 720, and 1440 eV. We realize that the simulations performed at high ion energy (720 and 1440 eV) represent less realistic magnetron sputtering conditions because, generally speaking, the ion energy during dc magnetron sputtering is of the order of 400 eV. We have used a much wider energy interval to study the influence of reactive ion implantation on the target condition in a more general way. The simulation results, i.e., the erosion rate as a function of the oxygen mole fraction, are presented in Fig. 1.

Due to the compound formation, which reduces the average sputter yield of the target, we notice an overall decrease of the erosion rate as a function of the oxygen mole fraction. However, at a given critical mole fraction f_{cr}, we notice an abrupt change for the erosion rate. The abrupt drop is for the lowest energy only 1% of the erosion rate in metallic mode ($f = 0.0$) while at high energy we notice a drop of ~10%. This abrupt change of the erosion rate occurs in a very narrow reactive mole fraction interval (interval width Δf equals 5×10^{-4} for the lowest energy and 1×10^{-3} for the highest
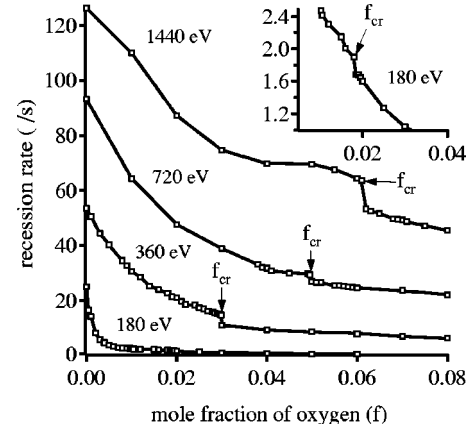

FIG. 1. Simulated erosion rate of an aluminum target as a function of the oxygen mole fraction f for different ion energies. The critical mole fraction is indicated by an arrow. The inset shows the erosion rate as a function of the oxygen mole fraction for the lowest ion energy, i.e., 180 eV.

energy). These results seem to confirm the proposed mechanism for the avalanche-like change of the target condition under influence of reactive ion implantation. A similar result was obtained with a version of an analytical model.[7] Meanwhile we have further improved this analytical model, and in the following, this model is described and its results compared with the TRIDYN results. In this way, we wish to verify the validity of this analytical model.

B. Analytical model: First version

At a given reactive gas mole fraction f, the steady state target condition can be described as a target composed of two materials having a strongly different sputter yield, i.e., the original target material with sputter yield γ_M and the compound formed by reactive ion implantation with sputter yield γ_c. Similar to the sputtering of alloys,[10] the target can be divided into a subsurface (b) and a surface (s) region with a different composition due to the difference in sputter yield of the two components. Of course, below these two defined regions the unaffected bulk target material is found. For both regions, i.e., the subsurface and surface region, we can define a degree of target reaction θ, which refers to mole fraction of compound MR_z in this region. The relation between the degree of target reaction for the subsurface region θ_b and the surface region θ_s can be described similar to the sputtering of alloys. In steady state, the amount of compound coming into the surface layer is $\theta_b v_s$ with v_s the erosion rate, defined as $[(1-\theta_s)\gamma_M + \theta_s\gamma_c](I)/n_o$, while the compound is removed from the surface at a rate equal to $\gamma_c\theta_s I$, with I the ion current density and n_o the target density. So the net rate of change for the compound in the surface layers is given by

$$n_{o,s}\frac{d\theta_s}{dt} = n_o\theta_b v_s - \gamma_c\theta_s I, \qquad (1)$$

with $n_{o,s}$ the target surface density (atoms/cm^2).
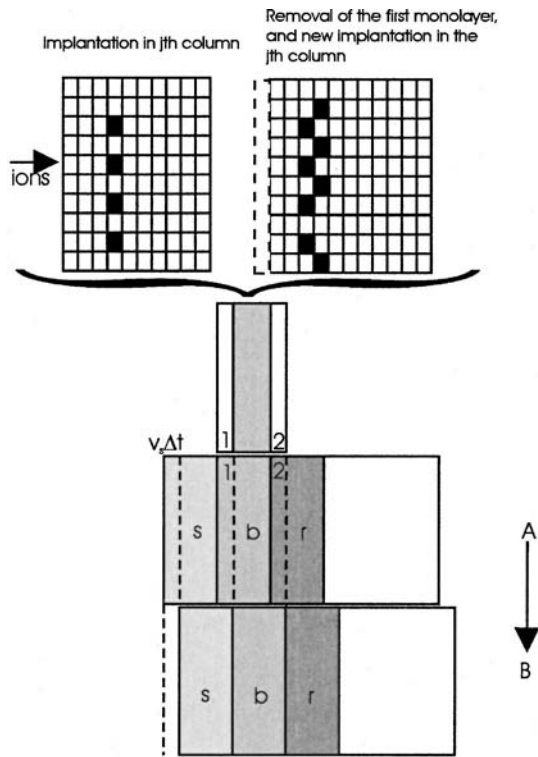
From Eq. (1), it follows that at steady state:

FIG. 2. Erosion of the target (situation A to B) over a distance $v_s \Delta t$ results in a material transfer from the subsurface region to the surface region (shaded region 1). In the layer r compound is formed by reactive ion implantation (shaded region 2). The erosion process can therefore be described using a two dimensional matrix N which represents the subsurface region. The black boxes, randomly chosen in the model, represent reacted target material with a sputter yield γ_C. After implantation of $2\,fA/\gamma_b$ reactive ions in the jth column (which corresponds with the shaded area 2), the first column is removed (shaded area 1), and to keep the dimensions of the matrix constant, a new empty column is added at the "backside" of this region.

$$\frac{\gamma_c \theta_s}{\gamma_M (1-\theta_s)} = \frac{\theta_b}{1-\theta_b}. \tag{2}$$

The steady state erosion rate can then be calculated as

$$v_s = \frac{I}{\left[\dfrac{(1-\theta_b)}{\gamma_M} + \dfrac{\theta_b}{\gamma_c} \right] n_o}. \tag{3}$$

In steady state, the compound formation by reactive ion implantation must compensate the compound sputter removal. In order to describe this process, we must consider not only the surface region s and the subsurface region b but, as shown in Fig. 2, also a third region r where the reactive ions become implanted and can react with the target material. As Fig. 2 demonstrates, the simultaneous sputter erosion and reactive ion implantation can be described as follows. The erosion of the target over a distance $\Delta s = v_s \Delta t$ results in a material transfer from the subsurface region b towards the surface region s. The ion bombardment of the target causing this target erosion results in the implantation of reactive ions into a layer with a thickness equal to $v_s \Delta t$. The implanted ions can react with the target material to form in steady state

a layer with a composition equal to the subsurface layer, i.e., the compound mole fraction must be equal to θ_b. Therefore, to describe this process we can consider only the subsurface region and represent this region by a two-dimensional matrix N. To remove one monolayer of this region, we must bombard the target with $A(1+z\theta_b)/\gamma_b$ ions, with A the number of rows in the two-dimensional matrix N and γ_b the average sputter yield in the subsurface region. The term $(1+z\theta_b)$ accounts for the increase in density due to the compound formation. Indeed, by the ion implantation the number of atoms to be sputtered increases so, z represents the number of R atoms needed to form the compound molecule MR_z. If f represents the mole fraction of reactive ions in the plasma, $2fA(1+z\theta_b)/\gamma_b$ of reactive atoms R become implanted in the target. Neglecting the implantation profile, we can assume that the R atoms become implanted in one column j of the two-dimensional matrix N. These R atoms will react with the target atoms, which is represented in this model by setting the value of $N_{i,j} = 1$, where i is randomly chosen for each implanted atom. As a target atom cannot react a second time with an implanted R atom the value of $N_{i,j}$ can only be 0 or 1, i.e., we assume that the R atom is lost for the chemical reaction if it encounters a matrix element $N_{i,j} = 1$. After implantation of $2fA(1+z\theta_b)/\gamma_b$ reactive atoms, we remove the first monolayer of the target, which is represented in this model by $N_{i,j+1} = N_{i,j}$. In this way, the implanted R atoms are shifted towards the target surface, where they modify the sputter yield, i.e., the sputter yield can be described as

$$\gamma_b = \gamma_M + (\gamma_c - \gamma_M)\theta_b$$

with

$$\theta_b = 1/A \sum_{i=1}^{A} N_{i,l}, \tag{4}$$

with γ_M the sputter yield of the metal and $\gamma_c (<\gamma_M)$ the sputter yield of the compound. Using the new value for the sputter yield γ_b we calculate again the number of reactive R atoms and the implantation process is repeated until the fraction θ_b of reacted target atoms in the first monolayer remains constant. Figure 3(a) (open symbols) shows the results of such a calculation using $\gamma_M = 0.5$, $\gamma_C = 0.05$, and $z = 1$. We clearly notice the abrupt change of the target condition at a critical mole fraction $f_{cr} = 0.065$.

For a further evaluation of this mechanism, we can describe the above-mentioned simple model more analytically. In steady state the amount of compound formed and removed should be equal. Or

$$\dot{F} = \dot{R}, \tag{5}$$

where $\dot{F}$ and $\dot{R}$ denote the formation and removal rate.

At steady state the first monolayer of the subsurface region contains in our simple model, $A\theta_b$ compound molecules. The time needed to remove this first monolayer depends on the erosion rate v_s, which is equal to $I\gamma_s/A$ with
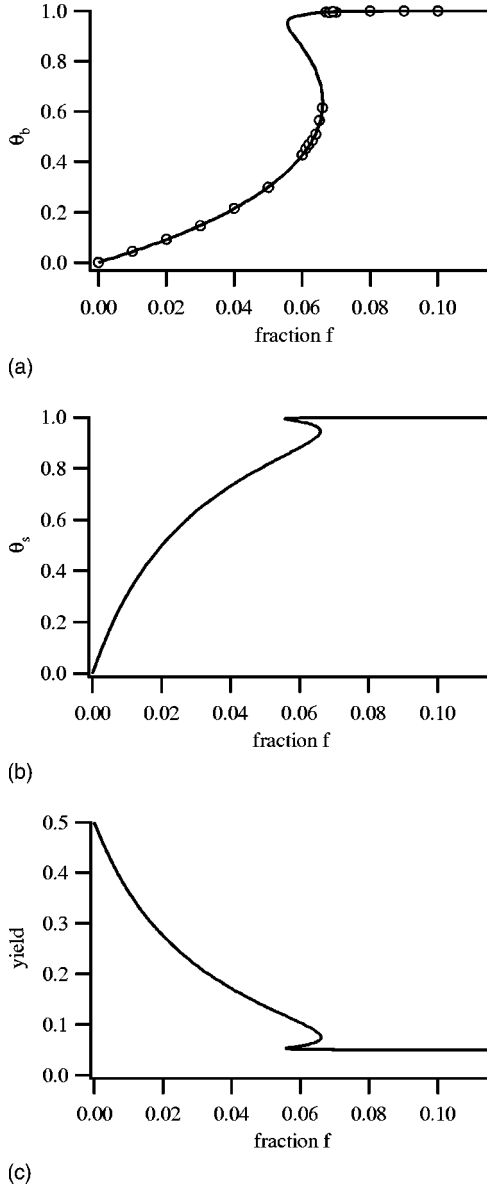
(a)

(b)

(c)

FIG. 3. Subsurface target condition as a function of the mole fraction f. The open symbols represent the result from the simple model using the matrix description of the subsurface region while the solid line represents the analytical approach summarized in Eq. (9) with $\gamma_M = 0.5$ and $\gamma_C = 0.05$, $z=1$ and $\alpha=1$; (b) calculated surface condition as a function of the mole fraction, using the same parameters as for (a); (c) calculated yield as a function of the mole fraction, using the same parameters as for (a).

γ_s the average sputter yield for the target surface, i.e., $\gamma_s = (1 - \theta_s)\gamma_M + \theta_s\gamma_c$. So, the removal rate $\dot{R}$ can be written as

$$\dot{R} = \frac{A\theta_b}{A/\gamma_s I} = \theta_b \gamma_s I. \tag{6}$$

From Eq. (1) as expected, it follows in steady state that $\dot{R} = \theta_s \gamma_c I$.

The implantation of a reactive atom R in column j of the target reduces the reaction probability for the next incoming R atom. This can be expressed as

TABLE I. Comparison of the critical mole fraction f_{cr} for the Al/O$_2$/Ar reactive sputtering system simulated with TRIDYN and calculated from the analytical model. In this latter calculation we have used the sputter yield for Al and Al$_2$O$_3$ given by TRIDYN taking into account the difference in sputter yield for O$^+$ and Ar$^+$ bombardment.

Ion energy (eV)	$f_{cr,\text{TRIDYN}}$	$f_{cr,\text{analytical}}$ [Eq. (9)]	$f_{cr,\text{analytical}}$ [Eq. (10)]
180	0.018	0.042	0.019
360	0.0299	0.085	0.042
720	0.0495	0.17	0.078
1440	0.061	0.21	0.10

$$\frac{d\theta_b}{dn} = \frac{\alpha}{zA}(1 - \theta_b), \tag{7}$$

with α the probability for reaction between R and a target atom and z the number of R atoms needed to form the compound molecule MR$_z$. The total number of implanted atoms per removed monolayer corresponds with $2\,fA(1 + z\theta_b)/\gamma_b$, which becomes implanted in a time interval $A/\gamma_s I$.

Therefore, the formation rate $\dot{F}$ equals

$$\dot{F} = \gamma_s I(1 - e^{-[(\alpha/z)2f(1+z\theta_b)/\gamma_b]}). \tag{8}$$

Combining Eq. (8) with Eqs. (5) and (6) results in an equation relating θ_b with f:

$$-\frac{z}{2\alpha}\frac{\ln(1 - \theta_b)[\gamma_M + \theta_b(\gamma_c - \gamma_M)]}{1 + z\theta_b} = f. \tag{9}$$

Choosing a value for θ_b the corresponding mole fraction f can be calculated and, as shown in Fig. 3(a) (solid line), this equation describes the simple model correctly. Using Eqs. (2) and (3), one can calculate from the value of θ_b, the surface composition θ_s [Fig. 3(b)] and the yield (or erosion rate v_s) [Fig. 3(c)].

As shown in Fig. 3(c), the behavior of the yield (or erosion rate) as a function of the mole fraction calculated from this analytical model is very similar to the results from the TRIDYN simulations. Using the sputter yields for both Al$_2$O$_3$ and Al calculated with the TRIDYN code, setting $z = 1.5\,(\text{Al}_2\text{O}_3)$ and $\alpha=1$, we can compare the results from this analytical model with the TRIDYN results. Such a comparison (see Table I) shows that the analytical model predicts larger values for the critical mole fraction than the TRIDYN simulations.

C. Analytical model: Second version

The strong deviation between the analytical model and the TRIDYN simulations can find its origin in several effects. Indeed, we realize that the analytical model neglects several effects, which are included in the TRIDYN code, i.e., knock-on implantation, range shortening, ion mixing, and others. However, these effects cannot, in our opinion, explain this strong deviation completely. Indeed, the major difference between the analytical model and the TRIDYN code is the approach of the chemical modification of the target. On the one hand, in the TRIDYN code the chemical reaction

between O and Al is actually not simulated. In this way, every incoming O atom results in a decrease of the sputter yield by affecting the surface binding energy matrix. On the other hand, in the analytical model, we assume that the reaction probability of the incoming O atoms is affected by the degree of reaction θ [see Eq. (7)], i.e., the higher the degree of reaction, the more O atoms are needed for a further poisoning of the target. In this way, the critical mole fraction is shifted towards larger values. To compare both models, we can modify the analytical model in the following way. When an implanted R atom encounters a matrix element $N_{i,j}=1$, we can choose a new random row i and repeat the implantation process, instead of assuming this atom is lost for the chemical modification of the target as in the first approach [Eq. (7)]. We can repeat this until the R atom encounters a matrix element $N_{i,j}=0$. Taking this approach into account, Eq. (9) becomes

$$\frac{z'}{2\alpha}\frac{[\gamma_M+\theta_b(\gamma_c-\gamma_M)]\theta_b}{1+z\theta_b}=f. \tag{10}$$

In the latter equation we have introduced two values for z, i.e., z and z'. Indeed, the difference in approach between the TRIDYN code and the analytical model also has an influence on the value of z, the number of reactive atoms needed to form one compound molecule MR_z. In the analytical model we have set $z'=1.5$ because 1.5 O atoms are needed to form one molecule of the compound, which has a different sputter yield compared to the target material. In the TRIDYN code, each implanted O atom influences the sputter yield by affecting the surface binding energy matrix, irrespective of the number of compound molecules formed. Therefore, to compare the result of the analytical model with the TRIDYN code we must set $z'=1$. However, the value of z in the denominator in Eq. (10), which accounts for the increase of atoms in the target (or density increase), remains equal to 1.5 as the maximum number of implanted O in TRIDYN is set equal to the number of O atoms in Al_2O_3. As shown in Table I, the critical mole fraction calculated using Eq. (10), approaches the TRIDYN values much better, especially for the low energy simulations. The erosion rate calculated from this analytical model, is compared in Fig. 4 with the result from TRIDYN at 360 eV.

Equation (10) predicts two interesting points, which are also reflected by the TRIDYN simulations. First, as the θ_b vs f curve is S shaped, Eq. (10) predicts [see also Figs. 3(a) and 4] hysteresis, i.e., when starting from a poisoned target, a lower reactive gas mole fraction must be used to return to the metallic state as compared to the inverse process.

Second, we can rewrite Eq. (10) as

$$\frac{z'}{2\alpha}\frac{\gamma_M[(1/r-1)\theta_b+1]\theta_b}{1+z\theta_b}=f, \tag{10'}$$

with r the ratio between the sputter yield of the target material and the compound, i.e., $r=\gamma_M/\gamma_c$. From the TRIDYN results, we learn that the ratio r is in the order of 10–30 depending on the ion energy. Under such conditions, Eq. (10′) predicts that the critical mole fraction should vary al-
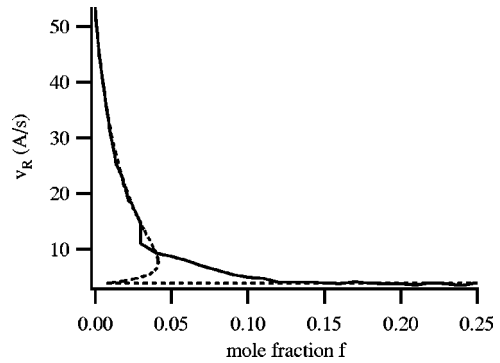

Fig. 4. Comparison between the erosion rates of an aluminum target calculated from the analytical model (dashed line) and the TRIDYN result at 360 eV (solid line). The erosion rate was calculated using Eq. (3), and the mole fraction using Eq. (10). We used the sputter yields and density for metal and compound as given by TRIDYN.

most linearly with the sputter yield of the metal. Using the TRIDYN model we can easily test these two predictions.

Figure 5 shows the linear relationship between the critical mole fraction f_{cr} and the sputter yield γ_M as calculated from the TRIDYN results. This behavior of the critical mole fraction as a function of the sputter yield of the target material can be easily understood from the analytical model. The number of implanted ions per removed monolayer is inversely proportional to the sputter yield, i.e., $2\,fA/\gamma_b$. Therefore, as the sputter yield of the target material increases, the critical mole fraction f_{cr} must increase proportionally to reach the same target condition.

In order to verify the hysteresis effect using the TRIDYN code, we have performed the simulation in the following way. After the calculation for $f=0.0$ (pure Ar bombardment) we used the output file describing the target condition as input file for the next calculation at $f=0.005$. This calculation was continued until $f=0.045$. Then using the same step $\Delta f=0.005$, we continued the calculation but now reducing the mole fraction until $f=0.0$. The result is shown in Fig. 6. As predicted from the analytical model, we notice the presence of hysteresis. Again this effect can be easily explained.
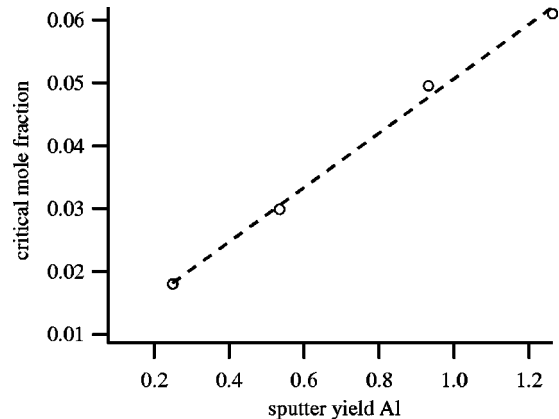

Fig. 5. Linear relation between the sputter yield of Al (calculated from the erosion rate at $f=0$ using TRIDYN) and the critical mole fraction fcr as shown in Fig. 1 (TRIDYN results). The dotted line is a linear fit.
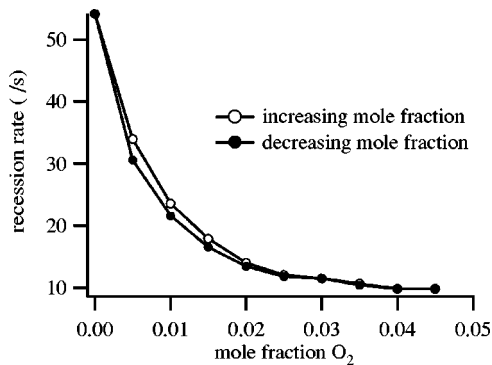
FIG. 6. TRIDYN hysteresis calculation at an ion energy of 360 eV for an aluminum target sputtered in an argon/oxygen mixture.

Starting from a metal target, we reduce the sputter yield by increasing the mole fraction of reactive gas in the plasma. At a given critical mole fraction the target becomes completely poisoned. At that point, the sputter yield equals γ_c, which is much lower than the sputter yield of the original target material and to remove one monolayer we must also implant a large number of reactive ions. In this way, the poisoned state can be maintained at lower mole fractions compared to the reverse process of reactive gas addition. From these results it follows that the hysteresis region is very narrow [see Fig. 3(a)] in agreement with our results presented in Ref. 3.

IV. CONCLUSION

In the TRIDYN simulation and in the analytical model, we use a known mole fraction of reactive gas. Therefore, we neglect the consumption of reactive gas by the sputtered target material, i.e., the gettering process. As shown by Berg *et al.*[9] the gettering process can, under certain experimental conditions, result in an abrupt change of the target condition and also hysteresis will be noticed. The simulations presented here, clearly show that an abrupt change of the target condition can also be induced by reactive ion implantation. Depending on the experimental conditions, this latter effect can be masked by the gettering process. Especially, at low pumping speed and high target current, the behavior of the target condition will be mainly dominated by the gettering process. However, under condition of high pumping speed and low target current, the ion implantation effects will be more pronounced, which is also true when the sticking coefficient of the reactive gas species on the target surface and deposited target material are low.

ACKNOWLEDGMENTS

[1] I. Safi, Surf. Coat. Technol. **127**, 203 (2000).
[2] D. Depla, A. Colpaert, K. Eufinger, A. Segers, J. Haemers, and R. De Gryse, Vacuum **66**, 9 (2002).
[3] D. Depla and R. De Gryse, Plasma Sources Sci. Technol. **10**, 547 (2001).
[4] D. Depla and R. De Gryse, Plasma Sources Sci. Technol. **11**, 91 (2002).
[5] D. Depla and R. De Gryse, Vacuum **69**, 529 (2003).
[6] Z. Y. Chen, A. Bogaerts, D. Depla, and V. Ignatova, Nucl. Instrum. Methods Phys. Res. B **207**, 415 (2003).
[7] D. Depla and R. De Gryse, Surf. Coat. Technol. (accepted for publication).
[8] W. Möller, W. Eckstein, and J. P. Biersack, Comput. Phys. Commun. **51**, 355 (1988); W. Möller and M. Posselt, TRIDYN FZR User Manual.
[9] S. Berg, H.-O. Blom, T. Larsson, and C. Nender, J. Vac. Sci. Technol. A **5**, 202 (1987).
[10] W. L. Patterson and G. A. Shirn, J. Vac. Sci. Technol. **4**, 343 (1968).